ISSN 1070-3284, Russian Journal of Coordination Chemistry, 2020, Vol. 46, No. 2, pp. 81–88. © Pleiades Publishing, Ltd., 2020.
Russian Text © The Author(s), 2020, published in Koordinatsionnaya Khimiya, 2020, Vol. 46, No. 2, pp. 73–80.

# Complexes $[Ni_2(\mu\text{-}OH_2)(\mu\text{-}O_2CCH(CH_3)_2)_2L_{2-4}((CH_3)_2CHCO_2)_2]$: Synthesis, Structure, and Mass Spectrometric Studies

**D. O. Blinou[a, *], A. A. Nikiforov[a, b], V. V. Gurzhiy[c], A. E. Minkovich[d], M. Yu. Maksimov[e], N. S. Panina[a], A. N. Belyaev[a], and A. V. Eremin[b, **]**

[a] *St. Petersburg State Institute of Technology (Technical University), St. Petersburg, Russia*
[b] *Institute of Macromolecular Compounds, Russian Academy of Sciences, St. Petersburg, Russia*
[c] *Institute of Earth Sciences, St. Petersburg State University, St. Petersburg, Russia*
[d] *Research Institute of Hygiene, Occupational Pathology, and Human Ecology, Federal Medical Biological Agency of Russia, St. Petersburg, Russia*
[e] *St. Petersburg Polytechnical University, St. Petersburg, Russia*
**e-mail: daniil.blinou@gmail.com*
***e-mail: ha9room@gmail.com*

Received July 11, 2019; revised August 11, 2019; accepted August 26, 2019

**Abstract**—Three new binuclear aqua-bridged nickel(II) 2-methylpropionate complexes $[Ni_2(\mu\text{-}OH_2)(\mu\text{-}O_2CCH(CH_3)_2)_2L_{2-4}((CH_3)_2CHCO_2)_2]$ (L is *N*,*N*,*N*',*N*'-tetramethylethylenediamine (**I**), pyridine (**II**), and 2,2'-bipyridyl (**III**)) are synthesized. The complexes are characterized by elemental and thermal analyses, mass spectrometry, IR and UV–Vis spectroscopy, and X-ray structure analysis (CIF files CCDC nos. 1840763 (**I**), 1913469 (**II**), and 1913471 (**III**)). The forms in which the synthesized coordination compounds exist in acetonitrile solutions are proposed on the basis of analyzing their mass spectra.

*Keywords:* polynuclear complexes, nickel, carboxylate ligands, structure, thermogravimetry, mass spectrometry, X-ray structure analysis

**DOI:** 10.1134/S1070328420020037

## INTRODUCTION

Transition metal complexes containing several coordination metal centers attract attention due to specific catalytic [1–3], magnetic [4–7], and spectral [8, 9] properties as well as a possible use in pharmacology [10, 11]. The binuclear complexes with bridging carboxylate ligands are among the most studied systems. A wide series of the binuclear nickel(II) complexes with aqua-, hydroxo-, or phenolate-bridging ligands [12–14] is interesting because these complexes resemble the active center the urease enzyme [15–18]. To the present time, several tens of the nickel(II) compounds with the $[Ni_2(\mu\text{-}OH_2)(\mu\text{-}O_2CR)_2L_2]^{2+}$ framework (L is the bidentate aminate ligand) were deposited with the Cambridge Crystallographic Data Centre (version 5.40, February 2019 [19]) [20–31]. When considering similar compounds as catalysts for homogeneous processes, it is important to study specific features of their behavior in solutions. However, this problem is insufficiently presented in the literature.

In this work, we studied the influence of the nature of the N-donor ligands in the binuclear nickel(II) complexes $[Ni_2(\mu\text{-}OH_2)(\mu\text{-}O_2CCH(CH_3)_2)_2L_{2-4}((CH_3)_2CHCO_2)_2]$ (L is *N*,*N*,*N*',*N*'-tetramethylethylenediamine (Tmeda for **I**), pyridine (Py for **II**), and 2,2'-bipyridyl (Bipy for **III**)) on the structures of the complexes, the character of thermal decomposition, and specific features of fragmentation in acetonitrile solutions.

## EXPERIMENTAL

All compounds and solvents were purchased from commercial sources and used as received. Synthetic hellyerite $NiCO_3 \cdot 5.5H_2O$ was obtained using the described procedure [32].

IR absorption spectra were recorded in a range of 400–4000 $cm^{-1}$ on a Shimadzu IRTracer-100 instrument equipped with a Specac Quest ATR accessory for attenuated total internal reflection (ATR). Electronic absorption spectra were measured on an SF-56 instrument using quartz cells ($l = 1$ cm). Elemental analyses for C, H, and N were carried out using a LECO CHNS(O)-932 analyzer.

Mass spectrometric analyses (ESI-MS) of solutions of the complexes were carried out on a TSQ Quantum Access Max instrument (Thermo Fisher Scientific). Solutions of the samples (0.1 mg/mL)

were introduced directly into electrospray with a flow rate of 10 μL/min. The voltages on the sprayer and capillary were ±5 kV and ±5 V, respectively. The pressure of the carrier gas (dry nitrogen) was 34.5 kPa, and the temperatures of the evaporator and capillary were 70 and 200°C, respectively. The spectra were recorded in the range of most intense signals: from 100 to 1000 Da.

The thermal decomposition of complexes **I–III** was studied by thermogravimetry (TG) on a Shimadzu DTG-60 analyzer. Experiments were carried out in dry nitrogen with a constant flow rate of 10 deg/min. The studied samples were heated in open aluminum crucibles, and the weight of each individual sample did not exceed 10 mg.

**Synthesis of μ-aqua-$k^2$O:O-di-μ-2-methylpropionato-$k^4$O:O'-bis[(2-methylpropionato-*k*O)(*N*,*N*,*N*',*N*'-tetramethylethylenediamine-$k^2$N,N')nickel(II)] [$Ni_2(\mu\text{-}OH_2)(\mu\text{-}O_2CCH(CH_3)_2)_2(Tmeda)_2((CH_3)_2\text{-}CHCO_2)_2$] (I).** 2-Methylpropionic acid (0.56 mL, 6 mmol) was added to a suspension of $NiCO_3 \cdot 5.5H_2O$ (0.6534 g, 3 mmol) in an acetonitrile–water (100 : 1) mixture (40 mL), and a solution of Tmeda (0.45 mL, 3 mmol) in acetonitrile (10 mL) was poured to the reaction mixture. Green crystals suitable for X-ray structure analysis precipitated from the mother liquor during slow evaporation in air. The yield of complex **I** was ~90%.

For $C_{28}H_{62}N_4O_9Ni_2$

| | | | |
|---|---|---|---|
| Anal. calcd., % | C, 47.04 | H, 8.75 | N, 7.84 |
| Found, % | C, 47.21 | H, 8.50 | N, 7.93 |

IR (ν, $cm^{-1}$): 3019 w, 2960 w, 2866 w, 2838 w, 2801 w, 2360 m, 2000 w, 1618 s, 1616 s, 1522 w, 1461 s, 1414 s, 1369 m, 1284 m, 1194 w, 1166 w, 1126 w, 1090 w, 1065 w, 1026 w, 958 w, 911 w, 827 w, 802 w, 775 w, 640 w, 618 w, 492 w.

**Synthesis of μ-aqua-$k^2$O:O-di-μ-2-methylpropionato-$k^4$O:O'-bis[(2-methylpropionato-*k*O)bis(pyridine-*k*N)nickel(II)] dihydrate [$Ni_2(\mu\text{-}OH_2)(\mu\text{-}O_2CCH(CH_3)_2)_2(Py)_4((CH_3)_2CHCO_2)_2] \cdot 2H_2O$ (II).** 2-Methylpropionic acid (0.75 mL, 8 mmol) was added to a suspension of $NiCO_3 \cdot 5.5H_2O$ (0.8711 g, 4 mmol) in an acetonitrile–water (100 : 1) mixture (50 mL), and a solution of Py (0.64 mL, 8 mmol) in acetonitrile (10 mL) was poured to the reaction mixture. Blue crystals suitable for X-ray structure analysis precipitated from the mother liquor during slow evaporation in air. The yield of complex **II** was ~85%.

For $C_{36}H_{54}N_4O_{11}Ni_2$

| | | | |
|---|---|---|---|
| Anal. calcd., % | C, 51.78 | H, 6.52 | N, 6.71 |
| Found, % | C, 51.93 | H, 6.22 | N, 6.82 |

IR (ν, $cm^{-1}$): 3436 w, 3075 w, 2964 w, 2924 w, 2866 w, 2325 w, 2102 w, 2051 vw, 1613 s, 1601 s, 1572 m, 1533 m, 1485 m, 1471 m, 1444 m, 1415 s, 1365 m, 1310 w, 1286 m, 1217 m, 1169 w, 1146 w, 1111 w, 1091 m, 1074 m, 1070 w, 1038 m, 1011 w, 919 w, 831 m, 759 m, 699 s, 651 m, 629 m, 566 m, 433 m.

**Synthesis of μ-aqua-$k^2$O:O-di-μ-2-methylpropionato-$k^4$O:O')-bis[(2-methylpropionato-*k*O)(2,2'-bipyridine-$k^2$N,N')nickel(II)][$Ni_2(\mu\text{-}OH_2)(\mu\text{-}O_2CCH(CH_3)_2)_2(Bipy)_2((CH_3)_2\text{-}CHCO_2)_2$] (III).** 2-Methylpropionic acid (1.12 mL, 12 mmol) was added to a suspension of $NiCO_3 \cdot 5.5H_2O$ (1.3068 g, 6 mmol) in an acetonitrile–water (100 : 1) mixture (40 mL), and a solution of Bipy (0.9364 g, 6 mmol) in acetonitrile (10 mL) was poured to the reaction mixture. Blue crystals suitable for X-ray structure analysis precipitated from the mother liquor during slow evaporation in air. The yield of complex **III** was ~80%.

For $C_{36}H_{46}N_4O_9Ni_2$

| | | | |
|---|---|---|---|
| Anal. calcd., % | C, 54.39 | H, 5.84 | N, 7.02 |
| Found, % | C, 54.50 | H, 5.52 | N, 7.23 |

IR (ν, $cm^{-1}$): 3114 w, 3037 w, 2961 w, 2921 w, 2866 w, 2066 w, 1979 w, 1899 w, 1612 s, 1605 s, 1569 m, 1531 w, 1495 w, 1478 m, 1469 m, 1442 m, 1414 s, 1366 m, 1357 m, 1322 m, 1308 w, 1285 m, 1250 w, 1168 w, 1151 m, 1113 w, 1088 m, 1058 m, 1026 m, 1018 w, 919 w, 829 m, 763 s, 736 s, 652 m, 632 m, 553 m, 448 w, 417 m.

**X-ray structure analyses** were carried out on an Xcalibur diffractometer (Rigaku Oxford Diffraction) equipped with an Eos CCD detector (Mo$K_\alpha$ radiation, λ = 0.71073 Å, graphite monochromator) at 100(2) K for complex **I** and on an XtaLab Supernova diffractometer (Rigaku Oxford Diffraction) equipped with a HyPix-3000 detector (Cu$K_\alpha$ radiation, λ = 1.54184 Å, mirror monochromator) at 100(2) K for complexes **II** and **III**. The structures of the compounds were solved by direct methods and refined using the SHELX programs [33] integrated in the OLEX2 complex [34]. The final models included the coordinates and anisotropic thermal parameters for all non-hydrogen atoms. The positions of the hydrogen atoms of the organic fragments of the molecules were calculated using the algorithm implemented in the SHELX program. The positions of the hydrogen atoms of the organic molecules were calculated using the algorithm implemented in the SHELX program package, where $U_{iso}$(H) was established as $1.5U_{eq}$(C) and C–H was 0.96 Å for the $CH_3$ groups, $U_{iso}$(H) was established as $1.2U_{eq}$(C) and C–H was 0.97 Å for the $CH_2$ groups, $U_{iso}$(H) was established as $1.2U_{eq}$(C) and C–H was 0.93 Å for the CH groups of the cyclic fragments, and $U_{iso}$(H) was established as $1.2U_{eq}$(C) and C–H was 0.98 Å for the tertiary CH group. The positions of the hydrogen atoms of the $H_2O$ molecules were localized from the difference Fourier synthesis and fixed during refinement with $1.5U_{eq}$(O). Note that the monoden-

**Table 1.** Crystallographic data and experimental and structure refinement parameters for complexes **I–III**

| Parameter | Value | | |
|---|---|---|---|
| | **I** | **II** | **III** |
| Empirical formula | $C_{28}H_{62}N_4Ni_2O_9$ | $C_{36}H_{54}N_4Ni_2O_{11}$ | $C_{36}H_{46}N_4Ni_2O_9$ |
| *FW* | 716.23 | 836.25 | 796.19 |
| Crystal system | Monoclinic | Triclinic | Triclinic |
| Space group | $P2_1/n$ | $P\bar{1}$ | $P\bar{1}$ |
| *a*, Å | 10.1209(10) | 9.34060(10) | 10.4484(5) |
| *b*, Å | 16.3044(18) | 20.83840(10) | 13.0505(7) |
| *c*, Å | 21.8566(19) | 21.9543(2) | 15.0916(7) |
| α, deg | 90 | 76.5040(10) | 77.525(4) |
| β, deg | 90.658(2) | 82.1540(10) | 84.004(4) |
| γ, deg | 90 | 89.3610(10) | 72.791(5) |
| *V*, Å$^3$ | 3606.4(6) | 4115.40(6) | 1917.49(18) |
| *Z*; $\rho_{calc}$, g/cm$^3$ | 4; 1.319 | 2; 1.350 | 2; 1.379 |
| *F*(000) | 1544 | 1768 | 836 |
| μ, mm$^{-1}$ | 1.095 | 1.636 | 1.691 |
| Index ranges | $-13 \le h \le 12$, $-21 \le k \le 21$, $-27 \le l \le 28$ | $-11 \le h \le 10$, $-25 \le k \le 25$, $-26 \le l \le 26$ | $-9 \le h \le 12$, $-15 \le k \le 15$, $-18 \le l \le 18$ |
| $2\theta_{max}$, deg | 54.996 | 143.776 | 139.99 |
| Number of measured/independent reflections | 8272/6559 | 16099/14310 | 5862/7257 |
| $R_{int}$ | 0.0237 | 0.0388 | 0.0501 |
| Number of parameters | 412 | 1015 | 471 |
| GOOF | 1.031 | 1.033 | 1.043 |
| $R_1$, $wR_2$ ($I > 2\sigma(I)$) | 0.0310, 0.0651 | 0.0662, 0.1718 | 0.0708, 0.1793 |
| $R_1$, $wR_2$ (all data) | 0.0462, 0.0728 | 0.0716, 0.1759 | 0.0867, 0.1931 |
| $\Delta\rho_{max}/\Delta\rho_{min}$, eÅ$^{-3}$ | 0.784/–0.432 | 1.059/–0.917 | 1.509/–0.639 |

tate 2-methylpropionate ligands in the structure of complex **II** were disordered over two crystallographically nonequivalent positions with a general population of 1.0. The crystallographic data and experimental and structure refinement parameters for complexes **I–III** are presented in Table 1.

The crystallographic data for complexes **I–III** were deposited with the Cambridge Crystallographic Data Centre (CIF files CCDC nos. 1840763 (**I**), 1913469 (**II**), and 1913471 (**III**); www.ccdc.cam.ac.uk/structures/).

## RESULTS AND DISCUSSION

Synthetic hellyerite $NiCO_3 \cdot 5.5H_2O$ was used as the initial compound in this work. The application of this compound allowed the fast syntheses in high yields of three new 2-methylpropionate complexes $[Ni_2(\mu\text{-}OH_2)(\mu\text{-}O_2CCH(CH_3)_2)_2L_{2-4}((CH_3)_2CHCO_2)_2]$ (L is Tmeda (**I**), Py (**II**), and Bipy (**III**)).

The molecular structures of complexes **I–III** are similar and have the binuclear framework in which two nickel atoms are linked to each other by the water molecule and two bidentate-bridging carboxylate ligands (Fig. 1). The coordination environment of each nickel ion is complemented by the 2-methylpropionate ligand coordinated via the monodentate mode and one bidentate N-donor ligand (Tmeda for **I** and Bipy for **III**) or two monodentate N-donor ligands (Py for **II**). The structures of complexes **I–III** are stabilized by intramolecular hydrogen bonds between the bridging water molecule and carboxylate ligands coor-

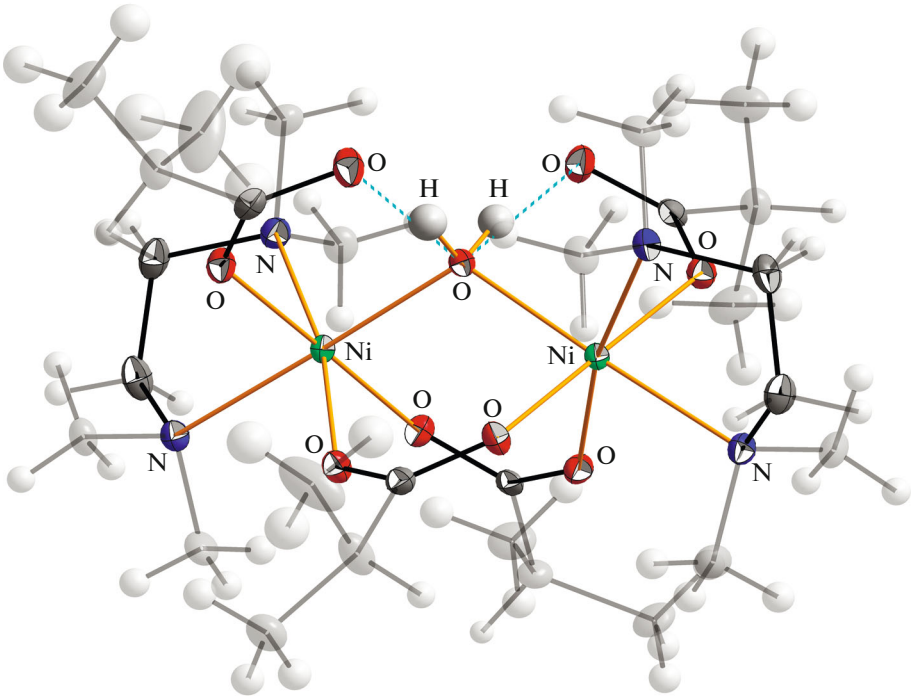


**Fig. 1.** Molecular structure of complex **I**. Intramolecular hydrogen bonds are shown. Thermal ellipsoids are given with 50% probability.

dinated via the monodentate mode. The lengths of the corresponding hydrogen bonds are presented in Table 2.

In the cases of complexes **I** and **III** containing the chelating bidentate ligands Tmeda and Bipy, a trapezoidal distortion of the equatorial plane of the coordination polyhedron is observed (Fig. 2). The concept on the so-called "continuous symmetry measures" S($O_h$) was used for the quantitative characterization of distortions of coordination polyhedra [35–37]. The value of continuous symmetry measures describes a deviation from the ideal octahedron shape: the higher the S($O_h$), the more appreciable the deviations. The calculation of S($O_h$) was performed by the X-ray structure data using the described algorithm [38]. For complexes **I**, **II**, and **III**, S($O_h$) was 0.2044, 0.0744, and 0.6117, respectively, which indicates that the most significant deviations are observed for complex **III**, whereas complex **II** is characterized by minimum deviations. This can be related to a higher structural rigidity of the Bipy ligand in the complex compared to that of Tmeda. In the case of the Py ligand, it cannot be excluded that its monodentate coordination mode assuming a higher flexibility of the metallic framework

**Table 2.** Main averaged bond lengths and bond angles in complexes **I–III**

| Parameter | Complex | | |
|---|---|---|---|
| | **I** | **II** | **III** |
| $O_W \cdots O_{carbox}$ | 2.547 | 2.563 | 2.539 |
| Ni···Ni | 3.480 | 3.557 | 3.503 |
| Ni–O(*w*) | 2.071 | 2.086 | 2.084 |
| Ni–N | 2.175 | 2.112 | 2.087 |
| $Ni–O_{\mu\text{-carbox}}$ | 2.033 | 2.042 | 2.043 |
| $Ni–O_{carbox}$ | 2.082 | 2.062 | 2.091 |
| NiO(*w*)Ni | 114.35 | 116.99 | 114.42 |
| NNiN | 84.13 | 89.07 | 78.70 |

*w* = $H_2O$, carbox = $O_2CCH(CH_3)_2$.

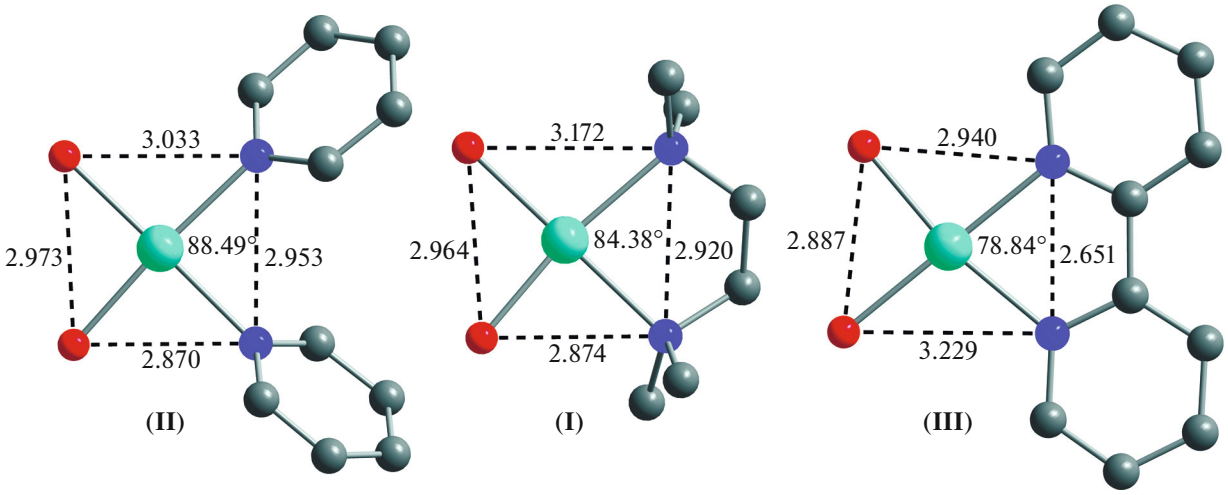


**Fig. 2.** Equatorial planes of the coordination polyhedra of complexes **I–III**. Carboxylate ligands and hydrogen atoms are omitted.

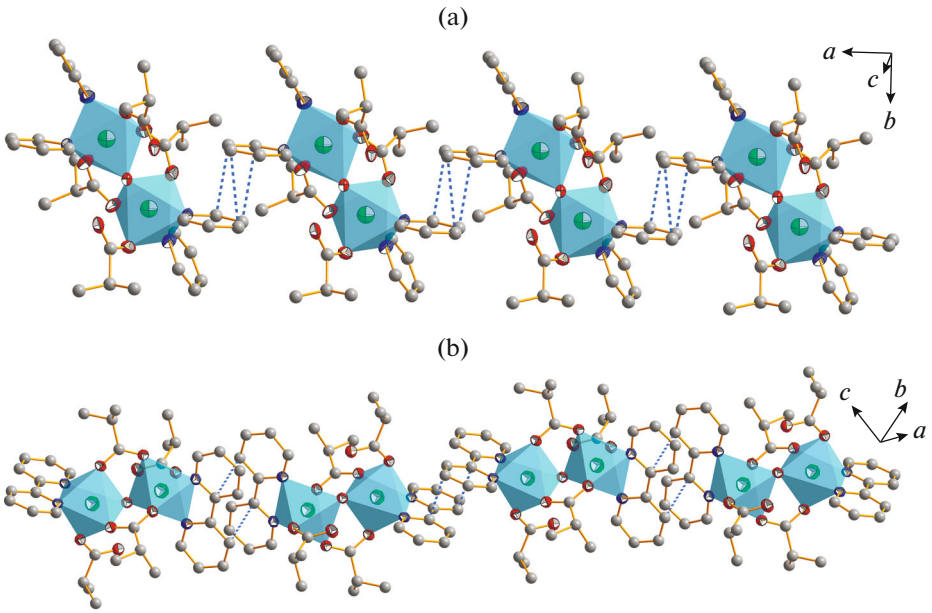


**Fig. 3.** Fragments of the crystal structures of complexes (a) **II** and (b) **III** with the stacking interactions. The coordination polyhedra $NiN_2O_4$ are shown.

results in the lowest distortion of the coordination polyhedra.

The π–π-stacking interactions of the aromatic ligands (Py and Bipy) leading to the formation of 1D polymer chains with average interplanar distances of 3.282 and 3.363 Å are observed in the crystal structures of complexes **II** and **III**, respectively (Fig. 3). The crystal structure of complex **II**, in addition to π–π interactions, contains a system of hydrogen bonds between monodentate coordinated carboxylate ligands and solvate water molecules.

In the IR spectrum of complex **II**, the weak and broad peak at 3436 $cm^{-1}$ indicates the presence of water of crystallization ($\nu_{as}$(O–H) and $\nu_s$(O–H)). The absorption bands in a range of 3100–2800 $cm^{-1}$ correspond to the ν(C–H) vibrations of the methylene and methyl groups of Tmeda (for **I**) and radicals of the carboxylate ligands (**I–III**). The intense absorption bands $\nu_{as}(COO^-)$ (1618 and 1616 for **I**, 1613 and 1601 for **II**, 1612 and 1605 $cm^{-1}$ for **III**) and the $\nu_s(COO^-)$ bands (1461 and 1414 for **I**, 1444 and 1415 for **II**, 1442 and 1414 $cm^{-1}$ for **III**) belong to the bridging and monodentate carboxylate ligands, respectively [39].

The nickel atoms exist in the distorted octahedral environment of $NiN_2O_4$ in complexes **I–III**. Three

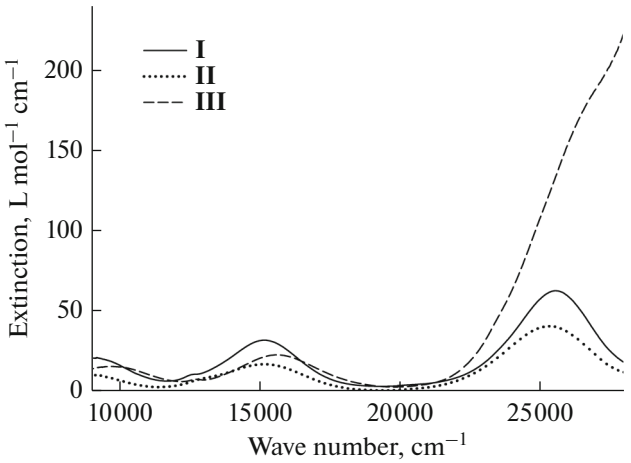


**Fig. 4.** Electronic absorption spectra of complexes **I–III** in acetonitrile solutions at room temperature.

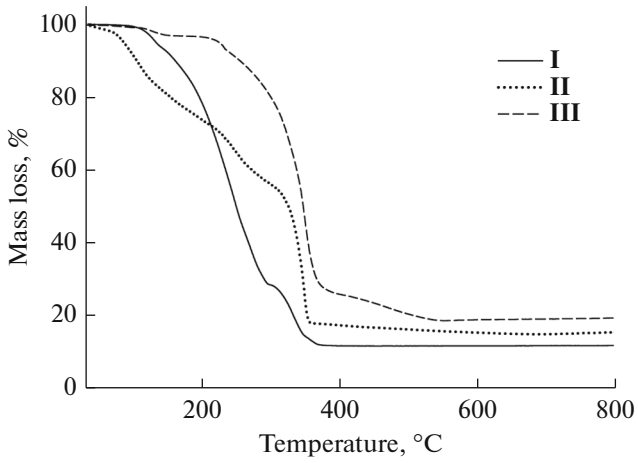


**Fig. 5.** TG curves for complexes **I–III**.

spin-allowed transitions $^3A_{2g} \rightarrow {}^3T_{2g}$, $^3A_{2g} \rightarrow {}^3T_{1g}$, and $^3A_{2g} \rightarrow {}^3T_{1g}(P)$ [40, 41] at 7000–13000, 11000–20000, and 19000–27000 cm$^{-1}$, respectively, appear in the visible range for similar octahedral and pseudo-octahedral $d^8$ systems. For complexes **I–III**, these transitions are observed at ~9500, ~15500, and ~26000 cm$^{-1}$, respectively (Fig. 4, Table 3). In the case of complex **III**, a significant increase of the molar extinction coefficient of the $^3A_{2g} \rightarrow {}^3T_{1g}(P)$ transition can be explained by the intraligand charge transfer in the developed aromatic Bipy–ligand system. The shoulder at ~13000 cm$^{-1}$ (Fig. 4) can be explained by the low-intensity spin-forbidden transition $^3A_{2g} \rightarrow {}^1E_g$ [40] observed at 12630(11), 12900(9), and 12750(7) cm$^{-1}$ (L cm$^{-1}$ mol$^{-1}$) for complexes **I–III**, respectively.

The study of the thermal behavior of complexes **I–III** showed that the thermal destruction of the complexes with the mono- (**II**) and bidentate (**I** and **III**) N-donor ligands proceeded via different routes. Complex **II** begins to decompose from the removal of outer-sphere water of crystallization, and this process ceases at 85°C ($\Delta m_{theor} = 4.31$, $\Delta m_{exp} = 4.87\%$). Then the combined consecutive elimination of the bridging water molecule and two pyridine molecules ($\Delta m_{theor} = 21.07$, $\Delta m_{exp} = 21.52\%$) is observed and possibly accompanied by the formation of compounds with the framework of the Chinese lantern type [21, 42]. Then two consecutive decomposition stages occur at 210–310 and 310–360°C to form nickel(II) oxide ($\Delta m_{theor} = 56.75$, $\Delta m_{exp} = 58.33\%$) (Fig. 5).

The TG curve of complex **I** exhibits a mass loss of 2.5% in a range of 100–120°C, which corresponds to the loss of the bridging water molecule. A sharp mass loss of 65.3% is observed in a range of 140–300°C. The total mass loss is 88.2% at the 20.9% (based on oxide) nickel content in the complex, indicating that the sublimation of the complex occurs in parallel to the thermal destruction processes.

The decomposition of complex **III** starts from the removal of the bridging water molecule in a range of 100–130°C. The further heating results in a sharp mass loss of the sample ($\Delta m_{exp} = 65.27\%$) in a range of 230–370°C. Two stages of the decomposition of the complex corresponding to the final destruction of the coordination polyhedra with the formation of NiO ($\Delta m_{theor} = 81.2$, $\Delta m_{exp} = 80.5\%$) are observed in a range of 370–540°C.

To obtain information about possible forms of the complexes in acetonitrile solutions, we studied them by mass spectroscopy. Both the positive and negative detection ranges of the ESI-MS spectra of an acetonitrile solution of complex **I** exhibit low-intensity peaks corresponding to the molecular ions $[M + H]^+$ ($m/z =$

**Table 3.** Assignment of the spin-allowed electronic transitions in complexes **I–III**

| Transition | ν, cm$^{-1}$ (ε, L cm$^{-1}$ mol$^{-1}$) | | |
|---|---|---|---|
| | **I** | **II** | **III** |
| $^3A_{2g} \rightarrow {}^3T_{2g}(F)$ | 9200 (22) | 9200 (10) | 10020 (15) |
| $^3A_{2g} \rightarrow {}^3T_{1g}(F)$ | 15190 (32) | 15170 (17) | 15700 (23) |
| $^3A_{2g} \rightarrow {}^3T_{1g}(P)$ | 25530 (63) | 25300 (41) | ~26600 (180) |

714.2, 1%) and $[M-H]^-$ ($m/z$ = 713.2, 1%). The ion corresponding to the mononuclear species $[Ni(Tmeda)((CH_3)_2CHCOO)]^+$ ($m/z$ = 261.1, 100%) has the highest intensity. Two peaks with $m/z$ = 567.2 (17%) and 609.2 (12%) are of lower intensity. The second peak can be assigned to the $[Ni_2(O_2CCH(CH_3)_2)_3(Tmeda)_2]^+$ ion.

A considerably higher number of peaks with high intensities corresponding to the "heavy" ions are observed in the mass spectra of complex **II**. The peaks with $m/z$ = 799.2 (20%) and 781.8 (38%) were ascribed to the molecular ion $[M + H]^+$ and its dehydrated form $[M-H_2O + H]^+$. In addition, two high-intensity peaks assigned to $[Ni_2(O_2CCH(CH_3)_2)_4(Py)_3 + H]^+$ ($m/z$ = 702.2, 100%) and $[Ni_2(O_2CCH(CH_3)_2)_4(Py)_3 + MeCN + H]^+$ ($m/z$ = 743.2, 75%) are observed. As in the case of complex **I**, the mononuclear species $[Ni(O_2CCH(CH_3)_2)_2(Py)_2 + H]^+$ ($m/z$ = 391.0, 36%) are detected in a solution of complex **II**. The dehydration of the complexes on the injection heated transfer line of the mass spectrometer can be one of the reasons for the absence of a water molecule in the structures of the most part of ions.

Thus, three new binuclear 2-methylpropionate complexes with the terminal N-donor ligands $[Ni_2(\mu\text{-}OH_2)(\mu\text{-}O_2CCH(CH_3)_2)_2L_{2-4}((CH_3)_2CHCO_2)_2]$ (L is Tmeda, Py, and Bipy) were synthesized. The observed deviations of the obtained compounds from the ideal octahedron shape were calculated on the basis of the X-ray structure analysis data. The structurally more rigid chelating bidentate ligands Bipy and Tmeda induce the highest trapezoidal distortions of the equatorial plane of the coordination polyhedra (**I** < **III**), whereas Py coordinated via the monodentate mode assumes a higher flexibility of the metallic core of complex **II** leading to the lowest distortion. The π–π-stacking interactions resulting in the formation of 1D polymer chains are observed in the crystal structures of the complexes with the aromatic Py and Bipy ligands.

The thermal destruction of complex **I** is accompanied by the sublimation of the compound. In the case of complexes **II** and **III**, NiO is the final decomposition product. Complex **II** loses the Py ligands in a range of 120–200°C and is isomerized to form the structures of the Chinese lantern type.

According to the ESI-MS spectra, the partial elimination of the carboxylate ligands with the formation of the $[Ni_2(O_2CCH(CH_3)_2)_3(Tmeda)_2]^+$ ions followed by their fragmentation to the mononuclear species $[Ni(Tmeda)((CH_3)_2CHCOO)]^+$ predominates in acetonitrile solutions of complex **I**. One Tmeda ligand is retained in the coordination environment of nickel in all identified ions. In the case of complex **II**, the main process is the elimination of one Py ligand to form the binuclear complex cations $[Ni_2(O_2CCH(CH_3)_2)_4(Py)_3 + H]^+$ and $[Ni_2(O_2CCH(CH_3)_2)_4(Py)_3 + MeCN + H]^+$ undergoing the consequent fragmentation to a lower extent than complex **I**. The absence of the bridging water molecule in the structures of the most part of ions can be explained by the loss of this molecule under the electrospray conditions.

## ACKNOWLEDGMENTS

The structural studies were carried out at the Resource Center "X-ray Diffraction Investigation Methods" of the Scientific Park of the St. Petersburg State University. The IR spectra were recorded and thermogravimetry was conducted at the Engineering Center of the St. Petersburg State Institute of Technology (Technical University).

## CONFLICT OF INTEREST

The authors declare that they have no conflicts of interest.

## REFERENCES

1. Long, J.M., Gao, H.Y., Liu, F.Sh., et al., *Inorg. Chim. Acta*., 2009, vol. 362, no. 9, p. 3035.
2. Wang, J.-W., Liu, W.-J., Zhong, D.-Ch., and Lu, T.-B., *Coord. Chem. Rev.*, 2019, vol. 378, p. 237.
3. Fischer, A.I., Panina, N.S., and Belyaev, A.N., *Russ. J. Coord. Chem*., 2016, vol. 42, no. 10, p. 635. https://doi.org/10.1134/S1070328416100018
4. Zorina-Tikhonova, E.N., Gogoleva, N.V., and Sidorov, A.A., *Polyhedron*, 2017, vol. 130, p. 67.
5. Malkov, A.E., Fomina, I.G., Sidorov, A.A., et al., *J. Mol. Struct.*, 2003, vol. 656, nos. 1–3, p. 207.
6. Novotortsev, V.M., Rakutin, Yu.V., Nefedov, S.E., and Eremenko, I.L., *Russ. Chem. Bull., Int. Ed*., 2000, vol. 49, no. 3, p. 438.
7. Nikolaevskii, S.A., Kiskin, M.A., Starikova, A.A., et al., *Russ. Chem. Bull., Int. Ed*., 2016, vol. 65, no. 12, p. 2812.
8. Das, M., Harms, K., Ghosh, B.N., et al., *Polyhedron*, 2015, vol. 87, p. 286.
9. Matelková, K., Boča, R., Dlhán, L., et al., *Polyhedron*, 2015, vol. 95, p. 45.
10. Bottari, B., Maccari, R., Monforte, F., et al., *Bioorg. Med. Chem.*, 2001, vol. 9, no. 8, p. 2203.
11. Bharty, M.K., Paswan, S., Dani, R.K., et al., *J. Mol. Struct.*, 2017, vol. 1130, p. 181.
12. Rispens, M.T., Gelling, O.J., de Vries, A.H.M., et al, *Tetrahedron*, 1996, vol. 52, no. 10, p. 3521.
13. Dey, S.K., Salah, El., Fallah, M., Ribas, J., et al., *Inorg. Chim. Acta*, 2004, vol. 357, no. 5, p. 1517.
14. Chang, C.-H., Tsai, C.-Y., Lin, W.-J., et al., *Polymer*, 2018, vol. 141, p. 1.
15. Sumner, J.B., *J. Biol. Chem.*, 1926, vol. 69, p. 435.
16. Blakeley, R.L., Treston, A., Andrews, R.K., and Zerner, B., *J. Am. Chem. Soc.*, 1982, vol. 104, no. 2, p. 612.
17. Blakeley, R.L. and Zerner, B., *J. Mol. Catal.*, 1984, vol. 23, nos. 2–3, p. 263.

18. Lippard, S.J., *Science*, 1995, vol. 268, no. 5213, p. 996.
19. Groom, C.R., Bruno, I.J., Lightfoot, M.P., and Ward, S.C., *Acta Crystallogr., Sect. B: Struct. Sci., Cryst. Eng. Mater.*, 2016, vol. 72, p. 171.
20. Eremenko, I.L., Golubnichaya, M.A., Nefedov, S.E., et al., *Russ. Chem. Bull., Int. Ed.*, 1998, vol. 47, no. 4, p. 704.
21. Eremenko, I.L., Nefedov, S.E., Sidorov, A.A., et al., *Inorg. Chem.*, 1999, vol. 38, no. 17, p. 3764.
22. Fomina, I.G., Sidorov, A.A., Aleksandrov, G.G., et al., *Russ. Chem. Bull., Int. Ed.*, 2004, vol. 53, no. 1, p. 114.
23. Denisova, T.O., Aleksandrov, G.G., Fialkovskii, O.P., and Nefedov, S.E., *Zh. Neorg. Khim.*, 2003, vol. 48, no. 9, p. 1476.
24. Mikhailova, T.B., Fomina, I.G., Sidorov, A.A., et al., *Zh. Neorg. Khim.,* 2003, vol. 48, no. 10, p. 1648.
25. Margossian, T. Larmier, K., Kim, S.M., et al., *J. Am. Chem. Soc*., 2017, vol. 139, no. 20, p. 6919.
26. Karmakar, A., Deka, K., Sarma, R.J., and Baruah, J.B., *Inorg. Chem.* Commun., 2006, vol. 9, no. 8, p. 836.
27. Karmakar, A., Sarma, R.J., and Baruah, J.B., *Eur. J. Inorg. Chem*., 2006, vol. 2006, no. 22, p. 4673.
28. Song, W.-D., Yan, J.-B., and Hao, X.-M., *Acta Crystallogr., Sect. E: Struct. Rep. Online*, 2008, vol. 64.
29. Singh, S., Saini, D., Mehta, S.K., and Choquesillo-Lasarte, D., *J. Coord. Chem.*, 2011, vol. 64, no. 9, p. 1544.
30. Qadir, A.M., *Asian J. Chem*., 2013, vol. 25, no. 15, p. 8829.
31. Walsh, J.P.S., Sproules, S., Chilton, N.F., et al., *Inorg. Chem.*, 2014, vol. 53, no. 16, p. 8464.
32. Bette, S., Rincke, C., Dinnebier, R.E., and Voigt, W., *Z. Anorg. Allg. Chem*., 2016, vol. 642, nos. 9–10, p. 652.
33. Sheldrick, G.M., *Acta Crystallogr., Sect. C: Struct. Chem.*, 2015, vol. 71, p. 3.
34. Dolomanov, O.V., Bourhis, L.J., Gildea, R.J., et al., *J. Appl. Crystallogr.*, 2009, vol. 42, p. 339.
35. Alvarez, S., Avnir, D., Llunell, M., and Pinsky, M., *New J. Chem.*, 2002, vol. 26, p. 996.
36. Alvarez, S., *Chem. Rev.*, 2015, vol. 115, no. 24, p. 13447.
37. Pavlov, A.A., Nikovskii, I.A., Polezhaev, A.V., et al., *Russ. J. Coord. Chem*., 2019, vol. 45, p. 402. https://doi.org/10.1134/S1070328419060046
38. The Continuous Symmetry Group. http://www.csm.huji.ac.il/new/.
39. Nakamoto, K., *Infrared and Raman Spectra of Inorganic and Coordination Compounds, Pt B: Applications in Coordination, Organometallic, and Bioinorganic Chemistry,* New York: Wiley, 2009.
40. Lever, A.B.P., *Inorganic Electronic Spectroscopy*, Amsterdam: Elsevier, 1984.
41. Meredith, P.L. and Palmer, R.A., *Inorg. Chem.*, 1971, vol. 10, no. 5, p. 1049.
42. Lee, D., Hung, P.-L., Spingler, B., and Lippard, S.J., *Inorg. Chem.*, 2002, vol. 41, no. 3, p. 521.

*Translated by E. Yablonskaya*